

N63-10795

NASA TN D-1396

NASA TN D-1396



# TECHNICAL NOTE

D-1396

AN ANALYSIS OF THE CONING MOTIONS OF THE FINAL STAGES OF  
THREE NASA SCOUT DEVELOPMENT VEHICLES

By George R. Young and James J. Buglia

Langley Research Center  
Langley Station, Hampton, Va.

NATIONAL AERONAUTICS AND SPACE ADMINISTRATION  
WASHINGTON

December 1962

NATIONAL AERONAUTICS AND SPACE ADMINISTRATION

TECHNICAL NOTE D-1396

AN ANALYSIS OF THE CONING MOTIONS OF THE FINAL STAGES OF  
THREE NASA SCOUT DEVELOPMENT VEHICLES

By George R. Young and James J. Buglia

SUMMARY

A simplified analysis has been used to study the coning motions produced by separation disturbances of the final stages of three NASA Scout development vehicles. Normal, longitudinal, and transverse accelerometers, magnetometers, and antenna patterns, along with radar data, were utilized in the study.

The results are given in terms of the calculated initial disturbing impulses required to give the stage a resultant flight-path deviation. The results indicated that Scout ST-2 received no discernible tipoff of the fourth stage, but Scouts ST-4 and ST-6 received initial disturbing impulses of at least 6.3 pound-seconds and 7.5 pound-seconds, respectively.

INTRODUCTION

One of the problems facing the designer of small, high-altitude research rocket vehicles is the problem of adequately stabilizing the attitude of the final stages of the vehicle which normally operate in near-vacuum conditions. Since these final stages are frequently too small to carry adequate reaction-control systems, many designers have used spin as a means of stabilization. The problem is then to separate cleanly the spinning final stage from the previous stage, which itself may or may not be spinning.

The NASA Scout vehicle is one of several vehicles which have experienced tipoff problems at the separation of a spinning stage. This report presents data describing the coning motion of the last stage of three Scout flights and the method used to derive these results from the information telemetered to ground receiving stations.

The results of this study were used to assist the designers in formulating a new separation system for the Scout. This new system has been tried on two flights and there is some indication that the separation impulse has been reduced to a satisfactory level.

## DESCRIPTION OF VEHICLE AND SEPARATION SYSTEM

The Scout is a four-stage, solid-fuel research vehicle nominally capable of placing about 150 pounds of payload into a 300-nautical-mile circular orbit. The motors are arranged in a tandem fashion with transition sections between the stages to tie the structure together and to provide space for instrumentation and controls. The complete configuration is about 72 feet long and weighs about 38,000 pounds at lift-off. A photograph of the ST-2 vehicle in the launching position is presented in figure 1, and a more complete description of the vehicle, its systems, and its performance capabilities is given in reference 1.

The first stage is controlled by means of a combination of aerodynamic and jet-vane controls; the second and third stages are controlled by means of small reaction motors. The guidance package, consisting essentially of a pitch programmer, miniature integrating gyros, and associated hardware, is located on top of the third stage.

The fourth stage of the Scout is spin stabilized and is separated from the third stage by means of a blast diaphragm. A schematic drawing of the separation of this diaphragm is shown in figure 2.

At a signal from the guidance timer, the spin motors are ignited and spin the fourth stage up to the required spin rate. At the same time, a 2-second delay squib is ignited. The squib fires the fourth-stage igniter, which produces sufficient pressure to collapse the diaphragm and free the spinning fourth stage.

## RESULTS AND DISCUSSION

There are indications (subsequently discussed) that at some time during the spin-up and separation sequence the fourth stage of two of the three Scout vehicles received an impulsive disturbance which caused the fourth stage to precess after separation. Thus the velocity increment added by the fourth stage did not lie along the nominal thrust axis but instead lay essentially along the axis of the precession cone swept out by the fourth stage, and hence the fourth stage was injected into orbit at the incorrect flight-path angle.

The equations necessary to analyze the precessional motion of a spinning stage from accelerometer data are derived in appendix B and are used in this study. The symbols used herein are defined in appendix A.

## Scout ST-2

The Scout ST-2 was launched from the NASA Wallops Station at 1023 hours e.s.t. on October 4, 1960. The purpose of this shot was to carry an 85-pound payload on a probe trajectory to an altitude of 3,100 nautical miles.

The onboard instrumentation pertinent to this study consisted of a magnetometer and normal and transverse accelerometers which measured accelerations in the body-fixed pitch and yaw planes. Telemeter traces of these three instruments during the time period of interest are shown in figure 3 along with a signal-strength record which was used as a check on the computation of the spin rate.

A detailed analysis of the Scout ST-2 telemeter record indicates that there was no discernible tipoff on that vehicle. The fact that only a slight tremor appeared in the accelerometer traces at the time of separation of the fourth stage indicated a relatively clean separation.

Since the magnetometer is fixed in the body, its trace gives a direct reading of the spin history. The time between successive peaks on the magnetometer trace was averaged over a number of cycles near ignition. From these data, it was estimated that the fourth stage of this vehicle was spinning at 143 rpm. A check on the spin rate was made by using the signal-strength data taken from ground receiving stations. Because of the antenna pattern produced by the ST-2, a direct reading of the spin rate was obtained here also and was found to be consistent with the rate obtained with the magnetometer.

By using the known radial distances from the spin axis of 3.98 inches and 3.88 inches for the normal and transverse accelerometers, respectively, their steady-state centrifugal accelerations were computed to be 2.33g and 2.27g. These values were in good agreement with the actual accelerometer readings corrected for zero shift. Time histories of the first few seconds of the normal and transverse accelerations determined from the telemeter record are shown in figure 4. Note that there is an apparent zero shift in both accelerometers, as they do not read zero g before spin-up. If the telemetered accelerations are corrected for zero shift, these accelerations agree well with the calculated steady-state accelerations, as shown in figure 4. Thus the accelerometers are functioning normally and the adjusted accelerations may be assumed to be correct.

There are several elements on the ST-2 telemeter trace (fig. 3) which indicate that there was no coning of this vehicle. These are pointed out and discussed separately to facilitate comparison with the traces from the other vehicles.

1. The normal and transverse accelerometers indicate that there was no coning after separation. If the vehicle were coning, as the result of an initial angular impulsive disturbance, there would be superimposed on this steady-state acceleration a sinusoidal acceleration whose frequency would be equal to the nutation frequency and whose amplitude would be proportional to the magnitude of the initial disturbance, as indicated in appendix C in equations (C19) and (C20). Within the reading accuracy of the telemeter trace (approximately  $\pm 0.05g$ ) no such motion can be detected for ST-2.

2. The magnetometer trace likewise indicates no coning. This instrument is mounted at an angle relative to the spin axis of the body and measures in effect the angle between the magnetometer axis and the earth's magnetic lines of force. The frequency shown on the magnetometer trace of figure 3 is thus exactly the spin frequency. If there were any coning present, the maximum amplitude of each wave of the magnetometer trace would change in a cyclic manner, and the envelope of these peaks would correspond to the precessional motion. The straight line labeled A drawn on the record indicates that there is no such motion discernible. The fact that the fourth stage is translating will not affect this argument since the direction of the magnetic lines of flux does not change appreciably during the few seconds in question.

3. The signal-strength record is obtained by measuring the strength of the telemeter signal on a ground receiver. The receiving antenna lies in a fixed plane. Since the airborne antenna is rotating relative to the ground antenna, it beats with the ground antenna one or more times per revolution, depending on the type of antenna pattern produced by the vehicle. The frequency of these beats is a direct indication of both the spin and the coning motions. In the case of Scout ST-2, the antenna pattern is such as to produce a record similar to that of the magnetometer. (See fig. 3(b).) The high-frequency curve shown on the record corresponds to the spin frequency. Any coning motion would superimpose on this trace a sine curve of lower frequency indicative of the coning motion. This motion does appear in the signal-strength data of Scouts ST-4 and ST-6, as is shown subsequently, but there is no indication of this motion on the Scout ST-2 signal-strength record.

#### Scout ST-4

The Scout ST-4 was launched from the NASA Wallops Station at 0805 hours e.s.t. on February 16, 1961. Its purpose was to place a payload of approximately 90 pounds into an orbit with nominal perigee and apogee altitudes of 360 and 1,500 nautical miles, respectively. The actual orbit had a perigee of 364 nautical miles and an apogee of 1,400 nautical miles.

Figure 5 is a photograph of the telemeter record obtained during the first few seconds of the fourth-stage burning period from this flight. The traces of interest on this flight are those of the single transverse accelerometer, two normal accelerometers, and the signal-strength record.

It has been determined from the orbital characteristics and the known injection time that the Scout ST-4 experienced an approximate  $1.8^\circ$  injection-angle error in the vertical plane. All third-stage radar tracking and telemeter data indicate that the final stage was essentially at the correct flight-path angle and attitude prior to spin-up and ignition. Hence, indications are that the injection-angle error must have arisen during the fourth-stage burning.

If the fourth stage were coning during burning, the velocity increment added by the fourth stage would be essentially along the center line of this cone. With an ignition velocity of approximately 15,000 feet per second and a fourth-stage velocity increment of about 10,000 feet per second, simple vector considerations indicate that the axis of this cone must have been at an angle of about  $4.5^\circ$  below the horizontal to produce a  $1.8^\circ$  injection-angle error. The total coning angle and hence the maximum deviation of the body-attitude angle  $\xi_{\max}$  was at least  $9^\circ$ .

There are three types of disturbance which could produce a coning motion, as discussed in reference 2 - thrust misalignment, dynamic unbalance, and a separation impulse. Approximate expressions for  $\xi_{\max}$  as a function of each of these disturbances are developed in appendix B and are given in equations (B29), (B31), and (B28), respectively.

The value of a constant disturbing moment  $N$  necessary to give a  $\xi_{\max}$  value of  $9^\circ$  can be calculated from equation (B29) by using Scout ST-4 parameters from the following table:

Roll moment of inertia, $I_x$ , slug-ft <sup>2</sup> . . . . .	6.25
Pitch and yaw moments of inertia, $I_y$ and $I_z$ , slug-ft <sup>2</sup> . . . . .	40.16
Roll rate, $p_0$ , radians/sec . . . . .	23.4
Thrust, lb . . . . .	3,500
Distance from center of gravity to nozzle exit, $r_e$ , ft . . . . .	3.25

This calculation results in  $N = 228$  foot-pounds, which for the thrust level and the center-of-gravity position  $r_e$  given in the table results from a thrust misalignment of  $1.34^\circ$ . In this calculation it is assumed that the moment due to the thrust misalignment is in such a direction as to place the axis of the resultant cone in the vertical plane. It is shown later that this could not be the case, and hence the thrust misalignment had to be greater than  $1.34^\circ$ .

If  $N = 228$  foot-pounds is substituted into equation (B30), the corresponding principal-axis misalignment angle  $\epsilon$  is found to be  $0.70^\circ$ .

If the initial angular velocity  $\omega_0$  which would produce the same cone angle from equation (B28) is considered,  $\omega_0 = 16.4^\circ$  per second.

The thrust misalignment and principal-axis misalignment required to produce the observed flight-path deviations are many times greater than those permitted in the specifications. Although this fact certainly cannot rule out the possibility of the occurrence of such large misalignments, they can, at least temporarily, be discounted as possible sources of external disturbance. In this case, however, separation impulse is about 3.5 pound-seconds, which is of the same order of magnitude as the separation impulses reported in reference 3. It remains to be determined whether a disturbance of this magnitude would produce time histories of normal and transverse acceleration consistent with those measured on ST-4.

If the only disturbance is assumed to be an initial angular rate  $\omega_0$ , the accelerations measured by the accelerometers mounted in a vehicle are given approximately by equations (C19) and (C20):

$$a_T = -y_T p_0^2 + x_T p_0 \frac{I_X}{I} \omega_0 \cos nt \quad (1)$$

$$a_N = -z_N p_0^2 - x_N p_0 \frac{I_X}{I} \omega_0 \sin nt \quad (2)$$

The first term in each of these equations is the steady-state acceleration produced by the fact that the accelerometer is not mounted on the center line but is mounted radially at a distance  $y_T$  or  $z_N$  from the center line. The second term is the acceleration produced by the initial angular velocity  $\omega_0$  for accelerometers mounted a distance  $x_N$  from the center of gravity. If there is no disturbance, the normal and transverse accelerations will be constants. This is the case shown in the ST-2 trace. The Scout ST-4, however, shows a sinusoidal wave superimposed on the normal- and transverse-accelerometer traces. (See fig. 5.) The magnitude of this sinusoidal term is found from the accelerometer trace to be about  $\frac{1}{8}g$ . The initial angular disturbance  $\omega_0$  is thus found from equations (1) and (2) to be about  $29^\circ$  per second. Since, from equation (B31), a disturbance of only  $16^\circ$  per second is required to account for the observed flight-path-angle change, the plane of the  $29^\circ$  per second disturbance must have lain between the planes of the normal and transverse

accelerometers at an angle of about  $56^\circ$  from the plane of the normal accelerometer. This disturbance of  $29^\circ$  per second could have been produced by a separation impulse of about 6.3 pound-seconds, which is considerably higher than the impulses reported in reference 3.

The record which most clearly shows that the vehicle was coning is the signal-strength record of figure 5. Again the high-frequency oscillations are a direct measure of the spin rate. The antenna used in this vehicle gave a figure-eight type of pattern, so that each two cycles on the record indicates one revolution of the vehicle.

The spin rate determined from the signal-strength record is 223 rpm. The low-frequency sine wave superimposed on the signal-strength trace is a direct measurement of the precession frequency. This frequency of 34 rpm agrees with the calculated precession frequency of 34.8 rpm.

The spin rate can also be calculated from the accelerometer traces. The high-frequency wave superimposed on the accelerometer trace has the nutation frequency. From equation (1) or (2),

$$n = \left(1 - \frac{I_X}{I}\right)p_0 = 189 \text{ rpm}$$

or  $p_0 = 223$  rpm, which is in agreement with the value calculated from the signal-strength record.

On the accelerometer records there is a violent disturbance at ignition and separation of the fourth stage which is visible in all the telemeter data. (Compare with the Scout ST-2 traces of fig. 3 at separation.) Unfortunately, the records are so scrambled for this time that there is no direct way of measuring this disturbance, and its magnitude must be inferred from the motion it produces, as was done previously.

There is also evident on the record of figure 5 some indication of binding between the third and fourth stages at separation. The fact that the normal and transverse accelerometer readings are slightly higher before separation than they are after separation indicates some loss of spin. The signal-strength data indicate that the spin rate was 225 rpm before separation and 223 rpm after, or a loss of about 2 rpm. This change in spin rate would produce a change in mean acceleration of 0.28g. The normal accelerometer shows a change of about 0.4g. The difference between the observed and calculated acceleration change, 0.12g, lies well within the accuracy band of the accelerometer,  $\pm 0.2g$ , so that the true binding effect is largely obscured by the accuracy of

L  
3  
0  
0  
9

the telemeter data. There is also the possibility that a zero shift occurred as a result of the separation bump.

#### Scout ST-6

The Scout ST-6 was launched from the NASA Wallops Station at 1329 hours e.s.t., August 25, 1961. Its purpose was to place a 127-pound micrometeorite satellite package into a slightly elliptical orbit with a perigee altitude of 245 nautical miles and an apogee altitude of 650 nautical miles. Orbital computations indicated, however, that the actual perigee altitude was about 75 nautical miles and that the final stage of the ST-6 was injected at a flight-path angle of about  $4^\circ$ , instead of the nominal  $0^\circ$ . Radar-tracking data and guidance-telemeter data indicated that the vehicle was on course and properly aligned up to fourth-stage ignition and separation. Once again it must be inferred that an erratic fourth stage was the cause of this large injection-angle error.

Unfortunately, Scout ST-6 had no payload instrumentation to telemeter to ground receiving stations any data on the motion of the final stage. The only data available on the fourth stage itself is a signal-strength record, shown in figure 6, which indicates that the fourth stage was indeed coning during burning. It is also estimated from this record that the fourth stage was spinning at about 175 rpm.

From the observed  $4^\circ$  injection-angle error, it is possible to proceed in a manner similar to that used in the ST-4 analysis. In order to produce the observed injection-angle error, the vehicle must have been describing at least a  $10^\circ$  half-angle cone, giving a  $\xi_{\max}$  value of at least  $20^\circ$ . A cone of this size would require that the fourth stage receive an angular disturbance (eq. (B31)), of at least  $37^\circ$  per second, caused by a separation impulse of at least 7.5 pound-seconds.

It must be emphasized that these are minimum numbers. That is, the assumption was made that the separation impulse produced only an initial yawing motion which produced a cone orientated in such a manner that the entire disturbance was felt as an error only in flight-path angle.

#### CONCLUDING REMARKS

A simplified analysis has been used to study the tipoff problems of three Scout development vehicles. This procedure utilized normal, longitudinal, and transverse accelerometers, magnetometers, and antenna

patterns, along with radar data, to study the motion of a spinning stage. The study indicated:

1. Scout ST-2 received no discernible tipoff of the fourth stage.
2. Scout ST-4 received an initial angular impulse of approximately 6.3 pound-seconds.
3. Scout ST-6 received an initial angular impulse of at least 7.5 pound-seconds.

Langley Research Center,  
National Aeronautics and Space Administration,  
Langley Station, Hampton, Va., June 21, 1962.

## APPENDIX A

## SYMBOLS

$a$	acceleration, ft/sec <sup>2</sup>
$a_p$	acceleration relative to center of gravity, ft/sec <sup>2</sup>
$b$	damping coefficient, $b'/I$
$b'$	pitch and yaw damping coefficient, $\dot{I} - \dot{m}r_e^2$
$F$	separation disturbing force, lb
$g$	constant of gravitational acceleration
$I = I_Y = I_Z$	
$I_X, I_Y, I_Z$	principal moment of inertia about body X-, Y-, and Z-axis, respectively, slug-ft <sup>2</sup>
$\vec{i}, \vec{j}, \vec{k}$	unit vectors in body-axis system
$K_1, K_2, K_3$	constants, defined by equations (B24), (B25), and (B26), respectively
$l$	distance from center of gravity to separation plane, ft
$M = N/I$	
$M_X = N_X/I_X$	
$M_Y = N_Y/I_Y$	
$M_Z = N_Z/I_Z$	
$m$	mass of body, slugs
$N$	moment about body axis
$N_X, N_Y, N_Z$	constant moment about body X-, Y-, and Z-axis, respectively, ft-lb

- $n$  nutation frequency,  $\left(1 - \frac{I_x}{I}\right)p_0$ , radians/sec
- $p, q, r$  component of body angular velocity about body X-, Y-, and Z-axis, respectively, radians/sec
- $r_e$  distance from body center of gravity to jet exit plane, ft
- $\vec{r}_p = \vec{i}x + \vec{j}y + \vec{k}z$
- $t$  time, sec
- $u, v, w$  component of velocity of center of gravity along body X-, Y-, and Z-axis, respectively
- $\vec{V} = \vec{i}u + \vec{j}v + \vec{k}w$
- $x, y, z$  coordinates in body-axis system
- $\kappa$  roll jet damping parameter
- $\epsilon$  principal-axis misalignment angle, radians unless otherwise indicated
- $\zeta = q + ir$
- $\xi = \theta + i\psi$
- $\phi, \theta, \psi$  roll, pitch, and yaw Euler angles, respectively
- $\vec{\omega} = \vec{i}p + \vec{j}q + \vec{k}r$
- $\omega_0$  initial angular rate, radians/sec unless otherwise indicated
- Subscripts:
- cg center of gravity
- max maximum
- N normal accelerometer
- o zero time

T            transverse accelerometer  
t            total acceleration on a particle  
X,Y,Z       direction of X-, Y-, and Z-axis, respectively

A dot over a symbol denotes a derivative with respect to time.

## APPENDIX B

## SIMPLIFIED EQUATIONS DESCRIBING THE BODY MOTION

In this appendix is presented a simplified analysis of the rotational motion of a rigid body whose mass and inertial properties are taken to be time invariant and which is acted upon by several disturbing parameters. Since only a very few seconds of the fourth-stage motion are analyzed, these approximate solutions can be used. More complete analyses of the motion of spinning, thrusting vehicles with variable mass and inertial properties can be found in references 2 and 4. Reference 5 is an interesting paper discussing the physics of spinning vehicles.

The standard Euler equations describing the motion of a rigid body (ref. 6), modified to include the jet damping terms, are:

$$I_X \dot{p} - (I_Y - I_Z)qr + \kappa p = N_X \quad (B1)$$

$$I_Y \dot{q} - (I_Z - I_X)rp + b'q = N_Y \quad (B2)$$

$$I_Z \dot{r} - (I_X - I_Y)pq + b'r = N_Z \quad (B3)$$

The following simplifying assumptions are made:

$$(1) \quad I_Y = I_Z = I, \quad \frac{I_X}{I} < 1.$$

(2) No roll damping or roll moment

Let  $b'$  be defined as

$$b' = \dot{I} - \dot{m}r_e^2 \quad (B4)$$

and define the damping coefficient  $b$  as

$$b = \frac{b'}{I} \quad (B5)$$

and

$$M = \frac{N}{I} \quad (\text{B6})$$

so that equations (B1) to (B3) can be written as

$$p = p_0 = \text{Constant} \quad (\text{B7})$$

$$\dot{q} - \left(1 - \frac{I_X}{I}\right)p_0 r + bq = M_Y \quad (\text{B8})$$

$$\dot{r} + \left(1 - \frac{I_X}{I}\right)p_0 q + br = M_Z \quad (\text{B9})$$

Now define

$$n = \left(1 - \frac{I_X}{I}\right)p_0 \quad (\text{B10})$$

$$\zeta = q + ir \quad (\text{B11})$$

$$M = M_Y + iM_Z \quad (\text{B12})$$

and write equations (B8) and (B9) as the single complex equation

$$\dot{\zeta} + (b + in)\zeta = M \quad (\text{B13})$$

which, if  $\zeta(0) = \zeta_0$  and  $b$  is constant, has the solution

$$\zeta = \frac{M}{b + in} + \left(\zeta_0 - \frac{M}{b + in}\right)e^{-(b+in)t} \quad (\text{B14})$$

The transformations from angular rates  $p$ ,  $q$ , and  $r$  about body axes to angular rates  $\dot{\phi}$ ,  $\dot{\theta}$ , and  $\dot{\psi}$  about space axes are given in reference 7 as

$$\dot{\phi} = p + q \sin \phi \tan \theta + r \cos \phi \tan \theta \quad (\text{B15})$$

$$\dot{\theta} = q \cos \phi - r \sin \phi \quad (\text{B16})$$

$$\dot{\psi} = q \sin \phi \sec \theta + r \cos \phi \sec \theta \quad (\text{B17})$$

If the assumptions of small angles for  $\theta$  and  $\psi$  and small rates for  $q$  and  $r$  are made, equations (B16) and (B17) may be combined as

$$\dot{\xi} = \dot{\theta} + i\dot{\psi} = \zeta e^{ip_0 t} \quad (\text{B18})$$

Substituting equation (B14) into (B18) and integrating, with  $\xi(0) = 0$ , gives

$$\xi = K_1 + K_2 e^{-bt} e^{i \frac{I_x}{I} p_0 t} + K_3 e^{ip_0 t} \quad (\text{B19})$$

where

$$K_1 = \frac{ip_0 \zeta_0 - M}{ip_0 [b + i(n - p_0)]} \quad (\text{B20})$$

$$K_2 = - \frac{\zeta_0 - \frac{M}{b + in}}{b + i(n - p_0)} \quad (\text{B21})$$

$$K_3 = \frac{1}{ip_0} \frac{M}{b + in} \quad (\text{B22})$$

Thus the motion in the  $\theta\psi$ -plane can be described by the sum of three vectors:

(1)  $K_1$  is a fixed vector.

(2)  $K_2 e^{-bt}$  is a vector, rotating at the angular velocity  $\frac{I_X}{I} p_0$ , whose magnitude is continually decreasing because of the jet damping. It is called the precession vector for  $\frac{I_X}{I} < 1$ .

(3)  $K_3$  is a vector, rotating at the angular velocity  $p_0$ , whose magnitude is constant. It is called the nutation vector for  $\frac{I_X}{I} < 1$ .

Note that this analysis gives a nutation frequency equal to the spin frequency. This erroneous result stems from the simplifying assumptions leading to equation (B18). As pointed out by Kolk in reference 8,  $p_0$  should be replaced by  $n$  in the  $K_3$  term of equation (B19), which then reads

$$\xi = K_1 + K_2 e^{-bt} e^{i \frac{I_X}{I} p_0 t} + K_3 e^{int} \quad (\text{B23})$$

Several special cases are now considered. Jet damping is neglected and it is assumed that the axes can be orientated in such a manner that  $r_0 = M_Z = 0$ . Then, equations (B20) to (B22) become

$$K_1 = \frac{-M_Y}{p_0(p_0 - n)} + i \frac{-q_0}{n - p_0} \quad (\text{B24})$$

$$K_2 = \frac{M_Y}{n(p_0 - n)} + i \frac{q_0}{n - p_0} \quad (\text{B25})$$

$$K_3 = - \frac{M_Y}{p_0 n} \quad (\text{B26})$$

The magnitude of the maximum value of  $\xi$ ,  $|\xi_{\max}|$ , can be expressed as

$$|\xi_{\max}| = |K_1| + |K_2| + |K_3| \quad (\text{B27})$$

Thus, if the disturbance is due to an initial pitching rate only,

$$|\xi_{\max}|_{q_0} = \frac{2q_0}{p_0} \frac{I_X}{I} \quad (\text{B28})$$

If the disturbance is a body-fixed moment  $N$ ,

$$|\xi_{\max}|_N = \frac{N}{I p_0^2} \frac{2}{\frac{I_X}{I} \left(1 - \frac{I_X}{I}\right)} \quad \left(\frac{I_X}{I} < 1\right) \quad (\text{B29})$$

where  $\frac{N}{I} = M$ .

A dynamic unbalance will produce a disturbing moment of the approximate magnitude

$$N = I p_0^2 \epsilon \left(1 - \frac{I_X}{I}\right) \quad (\text{B30})$$

where  $\epsilon$  is the principal-axis misalignment angle. (See ref. 2.) For this case, then,

$$|\xi_{\max}| = \frac{2\epsilon}{I_X/I} \quad (\text{B31})$$

## APPENDIX C

## ACCELERATIONS MEASURED BY THE ACCELEROMETERS

The total acceleration acting on a particle offset from the center of gravity is given by

$$\vec{a}_t = \vec{a}_{cg} + \vec{a}_p \quad (C1)$$

Now, in the rotating axis system

$$\vec{a}_{cg} = \vec{V} + \vec{\omega} \times \vec{V} \quad (C2)$$

where

$$\vec{V} = iu + jv + kw \quad (C3)$$

$$\vec{\omega} = ip + jq + kr \quad (C4)$$

The general expression for the acceleration of a particle relative to the moving system is given by

$$\vec{a}_p = \ddot{\vec{r}}_p + 2\vec{\omega} \times \dot{\vec{r}}_p + \dot{\vec{\omega}} \times \vec{r}_p + \vec{\omega} \times (\vec{\omega} \times \vec{r}_p) \quad (C5)$$

with

$$\vec{r}_p = ix + jy + kz \quad (C6)$$

For a particle fixed in the body,

$$\dot{\vec{r}}_p = \ddot{\vec{r}}_p = 0$$

so that, finally, equation (C1) becomes

$$\vec{a}_t = \dot{\vec{V}} + \vec{\omega} \times \vec{V} + \dot{\vec{\omega}} \times \vec{r}_p + \vec{\omega} \times (\vec{\omega} \times \vec{r}_p) \quad (C7)$$

Expanding equation (C7) gives, in component form,

$$a_{X,t} = \dot{u} - vr + wq - x(q^2 + r^2) - y(\dot{r} - pq) + z(\dot{q} + pr) \quad (C8)$$

$$a_{Y,t} = \dot{v} - wp + ur + x(\dot{r} + pq) - y(p^2 + r^2) - z(\dot{p} - qr) \quad (C9)$$

$$a_{Z,t} = \dot{w} - uq + vp - x(\dot{q} - pr) + y(\dot{p} + qr) - z(p^2 + q^2) \quad (C10)$$

Let the transverse accelerometer be located at  $(x_T, y_T, z_T)$  and measure  $a_{Y,t}$  and let the normal accelerometer be located at  $(x_N, y_N, z_N)$  and measure  $a_{Z,t}$ . Then equations (C9) and (C10) are written as

$$a_T = \dot{v} - wp + ur + x_T(\dot{r} + pq) - y_T(p^2 + r^2) - z_T(\dot{p} - qr) \quad (C11)$$

$$a_N = \dot{w} - uq + vp - x_N(\dot{q} - pr) + y_N(\dot{p} + qr) - z_N(p^2 + q^2) \quad (C12)$$

The accelerometers will be assumed to be orientated within the body so that  $z_T = y_N = 0$ .

If only the case of a disturbance produced by an initial pitching rate or yawing rate is considered, the first three terms on the right-hand side of equations (C11) and (C12) (the accelerations of the center of gravity) are zero, and these accelerometers will then read

$$a_T = x_T(\dot{r} + pq) - y_T(p^2 + r^2) \quad (C13)$$

$$a_N = -x_N(\dot{q} - pr) - z_N(p^2 + q^2) \quad (C14)$$

From equation (B14), if  $M_Y = M_Z = b = 0$ ,

$$q = q_0 \cos nt + r_0 \sin nt \quad (C15)$$

$$r = -q_0 \sin nt + r_0 \cos nt \quad (C16)$$

Since the only factor of interest here is the magnitude of the acceleration produced by the initial disturbance, and not whether it is produced by  $q_0$ ,  $r_0$ , or a combination of the two, the magnitude of this disturbance can be called  $\omega_0$  and equations (C15) and (C16) can be written

$$q = \omega_0 \cos nt \quad (C17)$$

$$r = -\omega_0 \sin nt \quad (C18)$$

If these expressions are substituted into equations (C13) and (C14), with the assumption that  $q, r \ll p$ , the result, after simplification, is

$$a_T = -y_{TP_0}^2 + x_{TP_0} \frac{I_X}{I} \omega_0 \cos nt \quad (C19)$$

$$a_N = -z_{NP_0}^2 - x_{NP_0} \frac{I_X}{I} \omega_0 \sin nt \quad (C20)$$

It can be seen that the disturbing angular rate  $\omega_0$  superimposes a sinusoidal acceleration on the steady-state acceleration of magnitude

$$x_{p_0} \frac{I_X}{I} \omega_0 \quad (C21)$$

and angular frequency

$$n = \left(1 - \frac{I_X}{I}\right) p_0 \quad (C22)$$

The expression (C21) is used to determine the magnitude of the initial angular disturbing rate  $\omega_0$ , and hence the disturbing impulse, since the quantity (C21) can be read from the accelerometer trace. The quantity (C22) can be used to check the spin rate  $p_0$  since the period of this oscillation can also be read from the telemeter record.

With the initial angular velocity  $\omega_0$  known, the angular disturbing impulse is given by

$$l \int F dt = I\omega_0 \quad (C23)$$

and hence the linear disturbing impulse is given by

$$\int F dt = \frac{I\omega_0}{l} \quad (C24)$$

where  $l$  is the distance from the center of gravity to the separation plane.

## REFERENCES

1. Mayhue, Robert J., compiler: NASA Scout ST-1 Flight-Test Results and Analyses, Launch Operations, and Test Vehicle Description. NASA TN D-1240, 1962.
2. Buglia, James J., Young, George R., Timmons, Jesse D., and Brinkworth, Helen S.: Analytical Method of Approximating the Motion of a Spinning Vehicle With Variable Mass and Inertia Properties Acted Upon by Several Disturbing Parameters. NASA TR R-110, 1961.
3. Gungle, Robert L., Brosier, William S., and Leonard, H. Wayne: An Experimental Technique for the Investigation of Tipoff Forces Associated With Stage Separation of Multistage Rocket Vehicles. NASA TN D-1030, 1962.
4. Martz, C. William: Method for Approximating the Vacuum Motions of Spinning Symmetrical Bodies With Nonconstant Spin Rates. NASA TR R-115, 1961.
5. Suddath, Jerrold H.: A Theoretical Study of the Angular Motions of Spinning Bodies in Space. NASA TR R-83, 1961.
6. Goldstein, Herbert: Classical Mechanics. Addison-Wesley Pub. Co., Inc. (Reading, Mass.), c.1950.
7. Abzug, Malcolm J.: Applications of Matrix Operators to the Kinematics of Airplane Motion. Jour. Aero. Sci., vol. 23, no. 7, July 1956, pp. 679-684.
8. Kolk, W. Richard: Modern Flight Dynamics. Prentice-Hall, Inc., 1961.

L  
3  
0  
0  
9



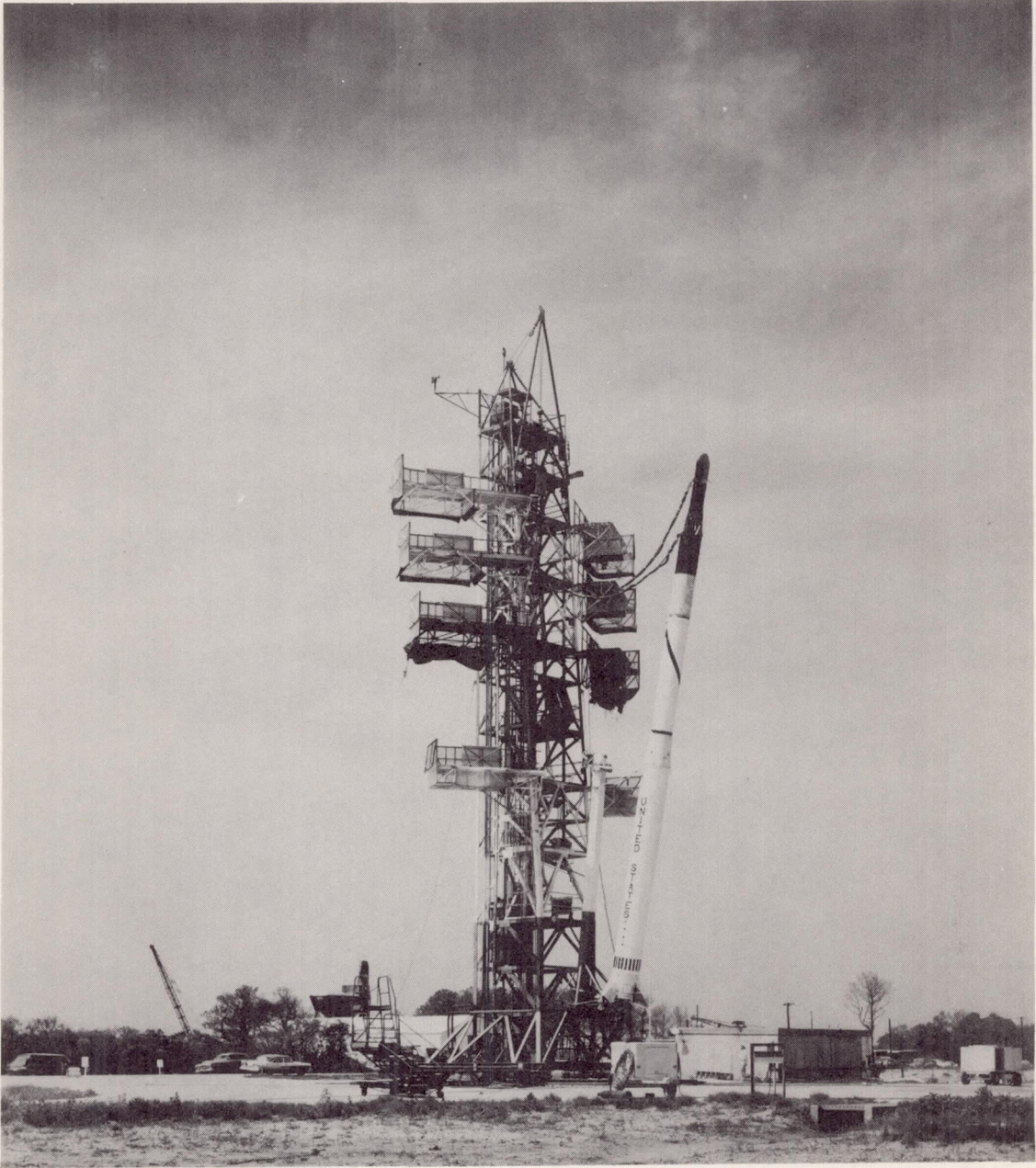


Figure 1.- Scout ST-2 test vehicle in launching position. L-60-3967

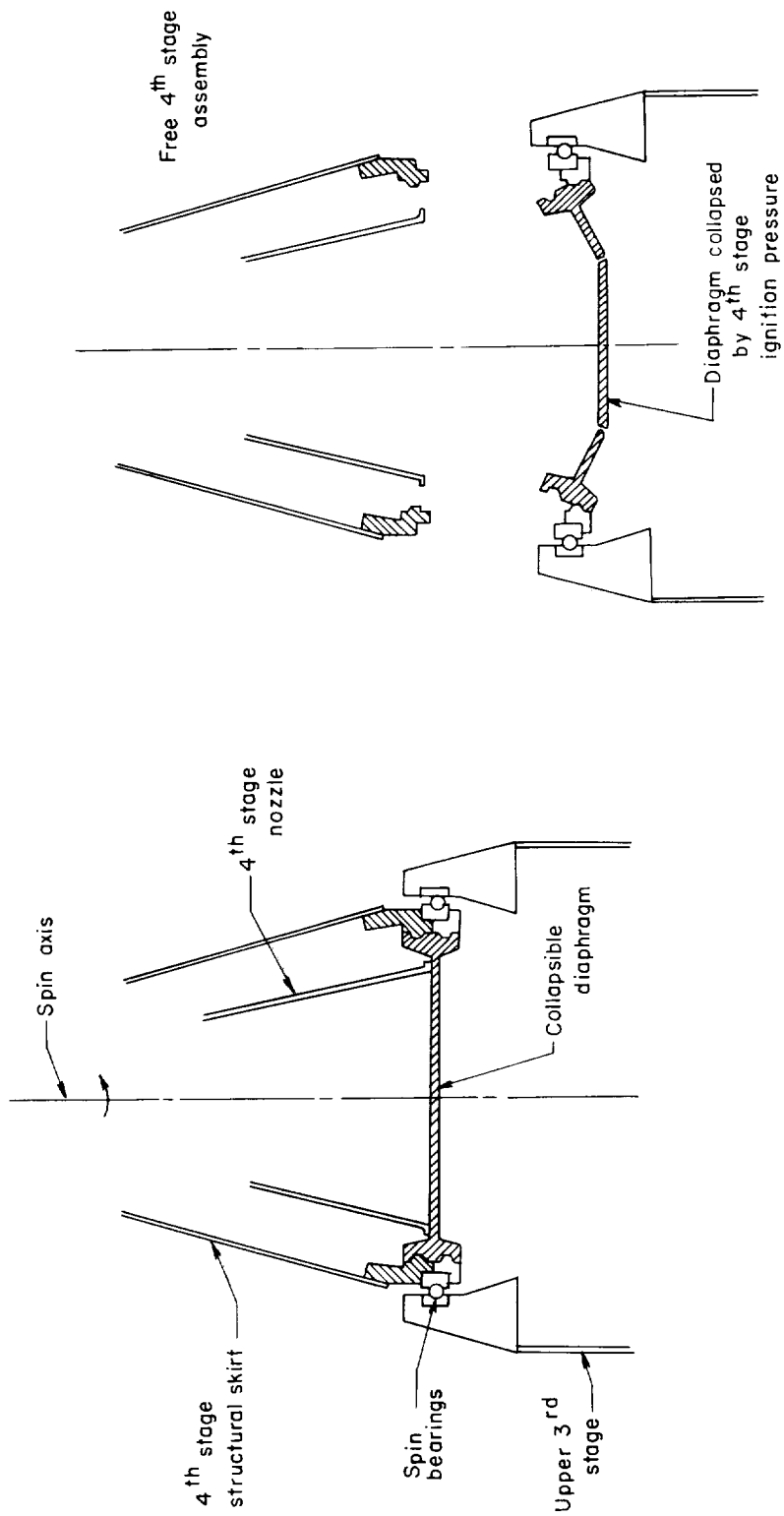
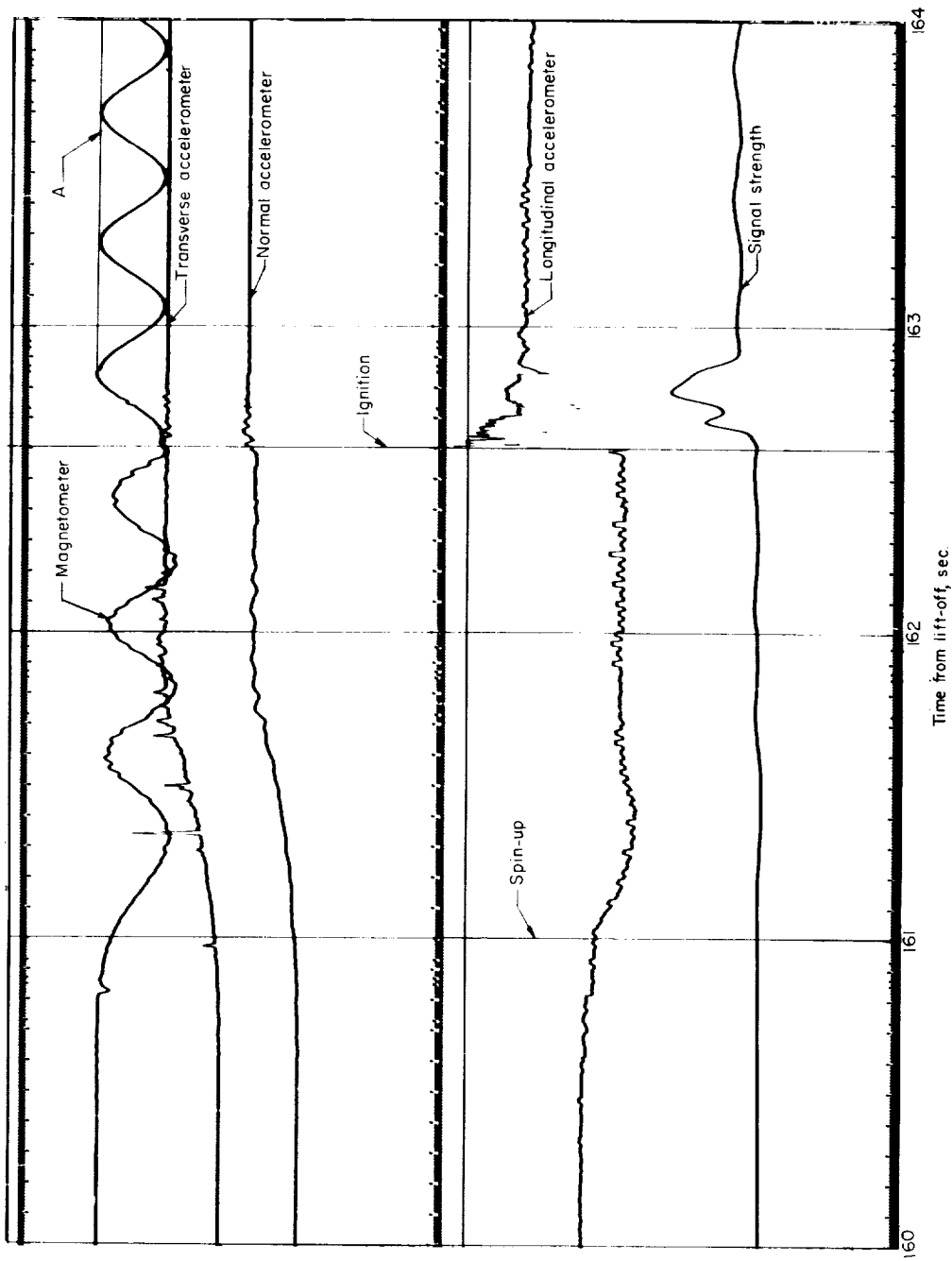
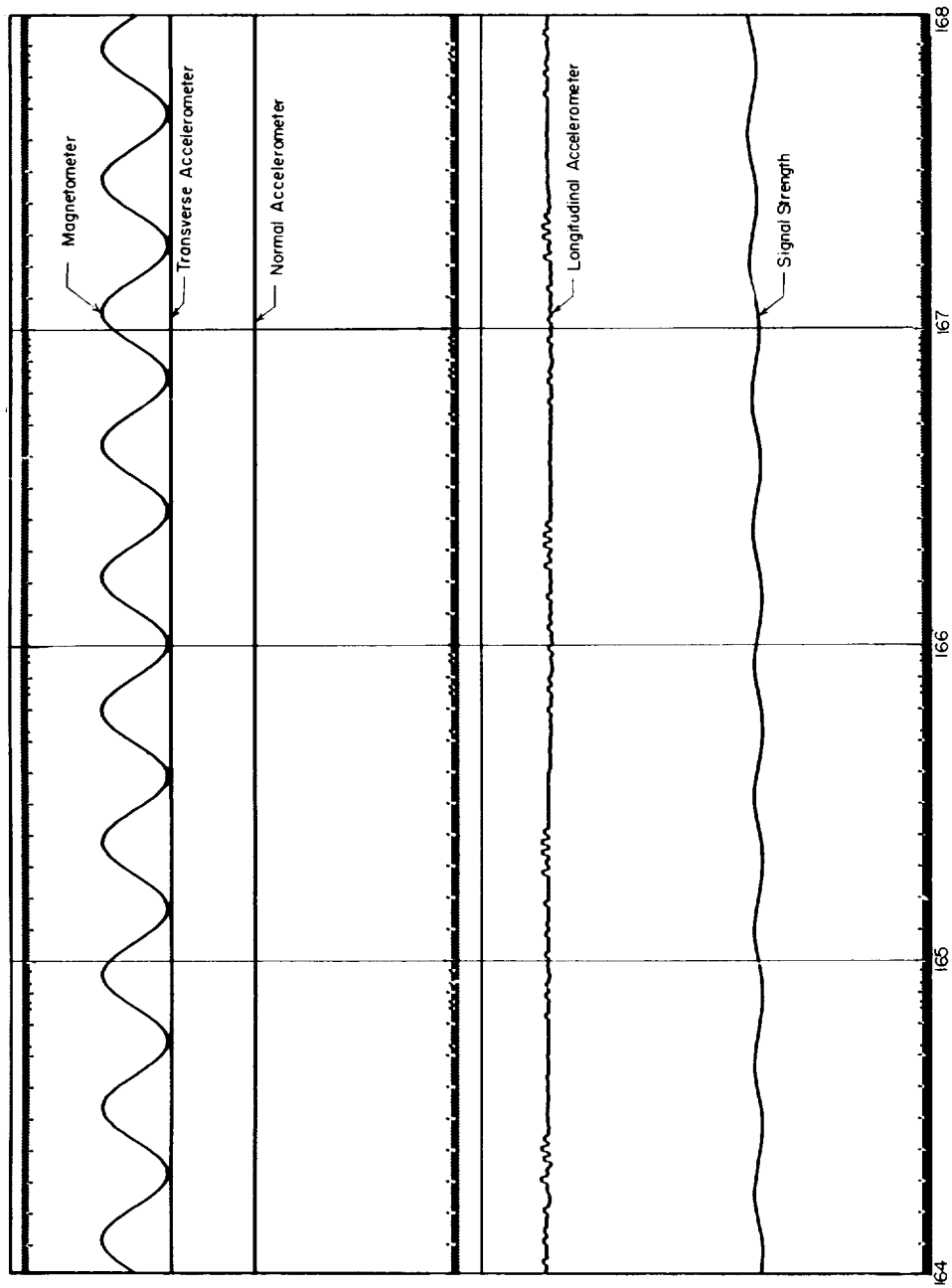


Figure 2.- Schematic showing diaphragm separation of fourth stage.



(a) 160 to 164 seconds.

Figure 3.- Telemetry data received during the early burning period of the fourth stage of Scout ST-2.



(b) 164 to 168 seconds.

Figure 3.- Concluded.

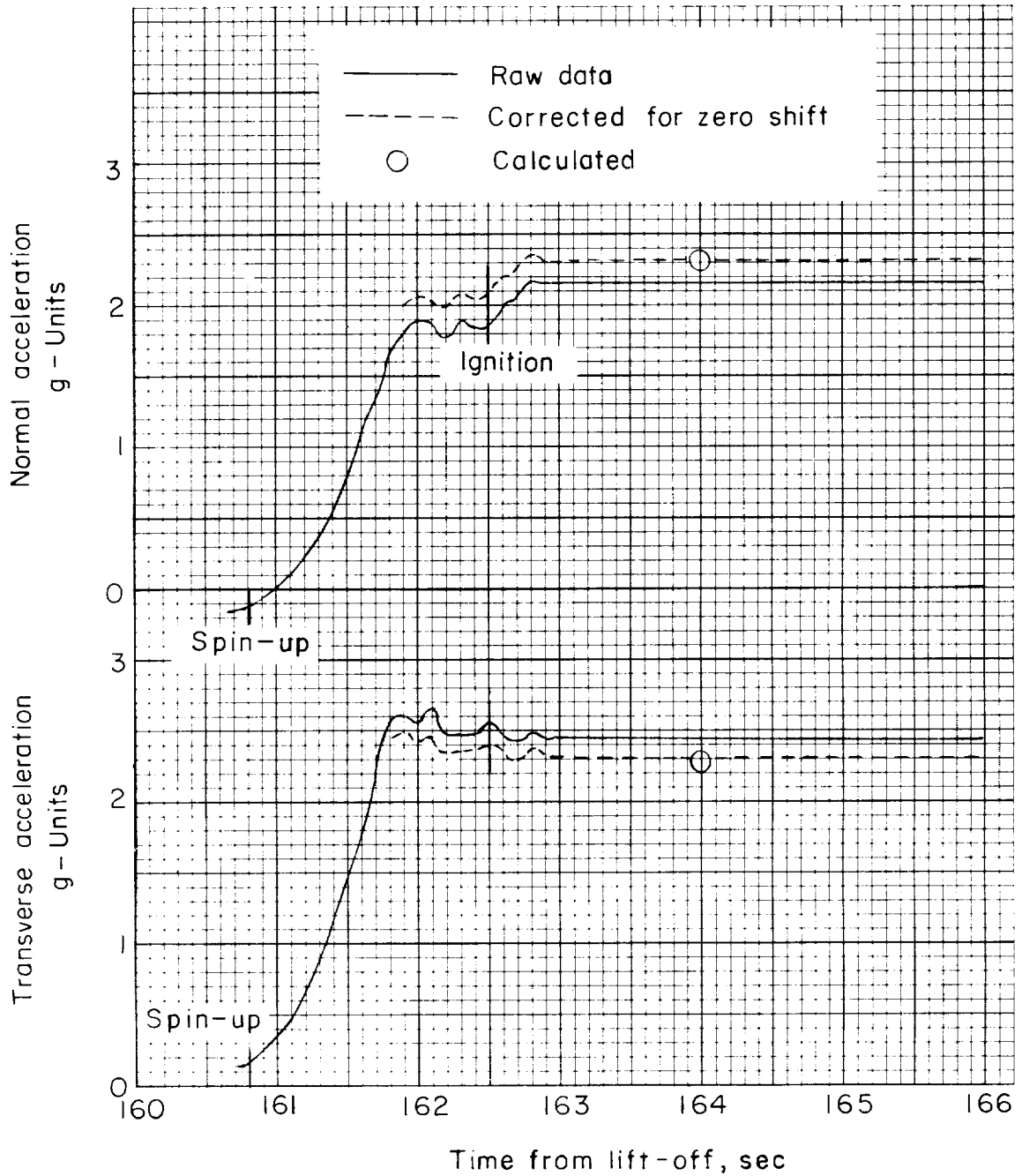


Figure 4.- Scout ST-2 normal- and transverse-accelerometer traces.

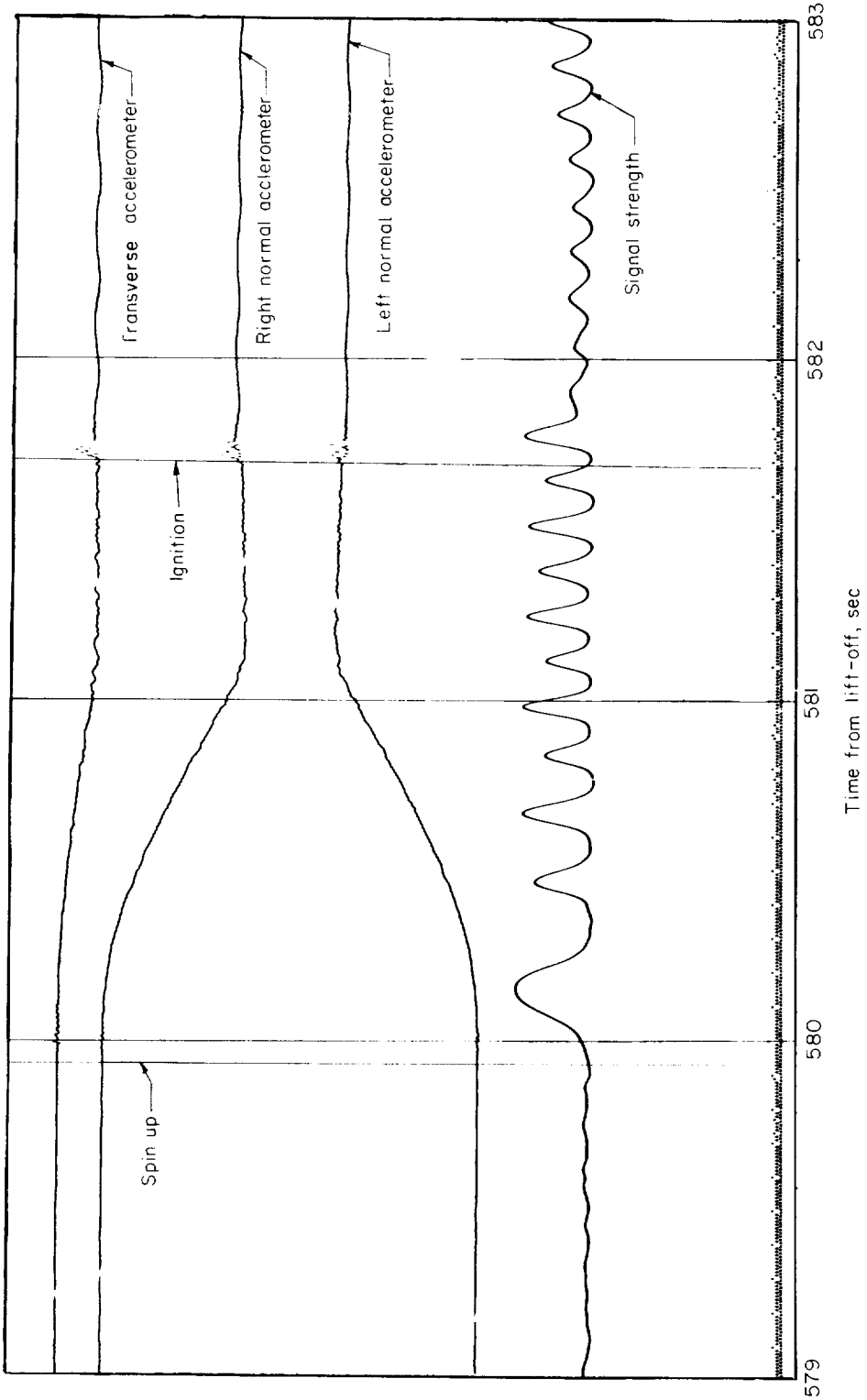


Figure 5.- Telemeter data received during the early burning period of the fourth stage of Scout ST-4.

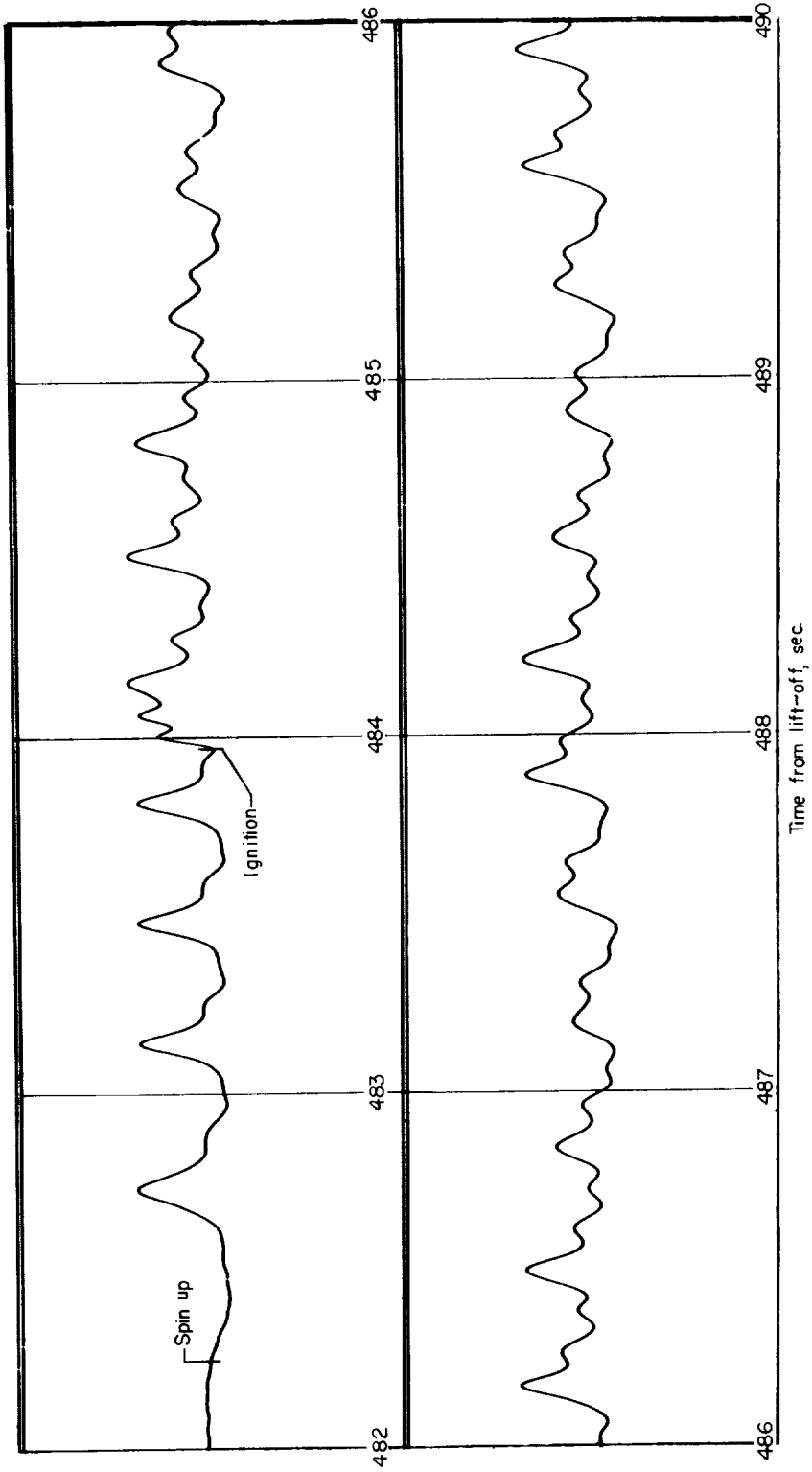


Figure 6.- Signal-strength record of Scout ST-6.